JACC Vol. 20, No. 4
October 1992:1005–16

Myocardial Contrast Echocardiography and the Transmural Distribution of Flow: A Critical Appraisal During Myocardial Ischemia Not Associated With Infarction

SANJIV KAUL, MD, FACC, ANANDA R. JAYAWEERA, PHD, WILLIAM P. GLASHEEN, PHD, FLORDELIZA S. VILLANUEVA, MD, HOWARD P. GUTGESELL, MD, FACC, WILLIAM D. SPOTNITZ, MD, FACC

Charlottesville, Virginia

Objectives. **This study was undertaken to determine whether myocardial contrast echocardiography can be used to estimate the transmural distribution of flow.**

Background. **Myocardial contrast echocardiography has been shown to reliably measure average transmural blood flow during myocardial ischemia. However, there is controversy regarding its ability to determine the transmural distribution of flow.**

Methods. **The transmural distribution of flow was measured in 21 open chest anesthetized dogs with use of radiolabeled microspheres and sonicated albumin microbubbles (mean size 4.5 μm). In the 11 Group I dogs, myocardial contrast echocardiography was performed at baseline and during left anterior descending artery stenosis. In five of these dogs, it was also performed during left circumflex artery stenosis. In these dogs large (mean 12 μm) hand-agitated bubbles were also used. In the five Group II dogs, myocardial contrast echocardiography was performed before and 45 s after intracoronary injection of 6 mg of papaverine in the presence of a critical left circumflex artery stenosis. The five Group III dogs were studied during cardiopulmonary bypass at baseline and during left anterior descending artery stenosis. Off-line image analysis of the echocardiographic images was performed and time-intensity curves obtained from these images were correlated with radiolabeled microsphere-derived flows.**

Results. **The ratios of the parameters derived from the endocardium and epicardium during myocardial contrast echocardiography were found to correlate poorly (ranging from $R^2 = 0$ to $R^2 = 0.35$) with radiolabeled microsphere-derived endocardial/epicardial flow ratios over a wide range of flow ratios (0.01 to 2.58). These results were not influenced either by the location of the regions of interest (left anterior descending vs. left circumflex artery bed) or by the size of the bubbles (4.5 vs. 12 μm).**

Conclusions. **Myocardial contrast echocardiography cannot be used to assess the transmural distribution of flow during myocardial ischemia not associated with infarction.**

(J Am Coll Cardiol 1992;20:1005–16)

Experimental data indicate that myocardial contrast echocardiography can be used to assess average transmural blood flow (1–6). However, there is controversy regarding the ability of this technique to determine the transmural distribution of flow in the context of myocardial ischemia (7–10). The present study was designed to determine whether this technique can be used to assess the transmural distribution of flow during acute myocardial ischemia in the absence of myocardial infarction. It was hypothesized that endocardial/epicardial flow ratios cannot be determined with use of this technique.

Because large bubbles (>12 μm) may get lodged within the myocardial arterioles (11), whereas small bubbles pass readily through the myocardial capillaries (11,12), we used both small and large bubbles to determine whether bubble size affects the ability of myocardial contrast echocardiography to assess endocardial/epicardial flow ratios. When the echocardiographic beam interrogates the anterior wall, the endocardium is more likely than the epicardium to be attenuated, whereas the epicardium is more likely to be attenuated when the beam interrogates the posterior wall. To resolve the issue of preferential attenuation, we imaged both beds.

Because cardiac motion due to rotation and respiratory

From the Division of Cardiology, Department of Medicine, the Division of Pediatric Cardiology, Department of Pediatrics and the Division of Thoracic and Cardiovascular Surgery, Department of Surgery, University of Virginia School of Medicine, Charlottesville, Virginia. This study was supported by grants-in-aid from the Virginia Affiliate of the American Heart Association, Glen Allen, Virginia (Drs. Kaul, Gutgesell, Spotnitz) and a grant-in-aid from the National Center of the American Heart Association, Dallas, Texas (Dr. Kaul). Drs. Kaul and Spotnitz are recipients of FIRST Awards from the National Institutes of Health, Bethesda, Maryland. Dr. Kaul is an Established Investigator of the American Heart Association. This work was presented in part at the 38th Annual Scientific Session of the American College of Cardiology, Anaheim, California, March 1989 and in part at the 39th Annual Scientific Session of the American College of Cardiology, New Orleans, Louisiana, March 1990.

The microbubbles and radiolabeled microspheres used in this study were provided, respectively, by Molecular Biosystems, San Diego, California and Dupont Medical Products, North Billerica, Massachusetts.

Manuscript received January 10, 1992; revised manuscript received April 2, 1992, accepted April 8, 1992.

Address for correspondence: Sanjiv Kaul, MD, Box 158, Division of Cardiology, University of Virginia School of Medicine, Charlottesville, Virginia 22908.

0735-1097/92/$5.00

translation can influence echocardiographic data analysis, we also performed myocardial contrast echocardiography during cardiopulmonary bypass when the heart is arrested and there is no cardiac translation caused by respiration. In this situation every frame can be analyzed without having to be aligned with each other, thus increasing both the temporal resolution of the data and the accuracy of data registration between frames. To enhance the signal to noise ratio, we utilized image depths to maximize the size of the regions of interest. For optimal registration between microsphere and echocardiographic data, we used postmortem flow maps generated by injecting colored dye into the myocardial bed.

Methods

Animal preparation. Twenty-one mongrel dogs were used for these experiments. The studies conformed to the "Position of the American Heart Association on Research Animal Use" adopted November 11, 1984 by the American Heart Association. The dogs were anesthetized with 30 mg/kg body weight of intravenous sodium pentobarbital (Abbott) and intubated and ventilated with a respirator pump (model 607, Harvard Apparatus). An 8F catheter was placed in the left femoral artery for recording arterial pressure and was connected to a multichannel physiologic recorder (model 4568C, Hewlett-Packard) by way of a fluid-filled transducer (model 1280C, Hewlett-Packard). This catheter was also used for the withdrawal of reference arterial blood samples during injection of radiolabeled microspheres into the left atrium in Group I and Group II dogs. A similar catheter was placed in the left femoral vein for the administration of drugs and fluids, as needed. Two mg/kg of lidocaine hydrochloride was injected intravenously and followed by an infusion of 2 mg/min throughout the experiment. Arterial blood gases were monitored every hour and the concentration of inspired oxygen was adjusted and sodium bicarbonate (Abbott) was given accordingly. The chest was opened and the heart was suspended in a pericardial cradle.

Group I dogs (n = 11). A 4F catheter was placed in the left atrium for the injection of radiolabeled microspheres and the left main artery was dissected free from surrounding tissues and a silk tie was placed loosely around it. A hydraulic occluder was positioned on the proximal left anterior descending artery, and a 22-gauge catheter was placed in the lumen of this artery to measure pressure beyond the occluder (Fig. 1). In five dogs an occluder was also positioned on the left circumflex artery. An electromagnetic flow probe (model EP406, Carolina Medical) was placed proximal to the occluder (Fig. 1) to measure flow through this vessel and was connected to a flow meter (model FM502, Carolina Medical) that in turn was connected to the physiologic recorder.

The right carotid artery was exposed and a 12F cannula (Bardic) was placed in it. This cannula was connected to plastic tubing (Tygon) placed in a constant flow roller pump (Series S, Manostat) and the other end of the tubing was

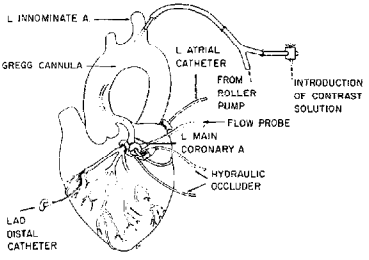

Figure 1. Animal preparation used for Group I dogs (see text for details). A. = artery; L. = left; LAD = left anterior descending coronary artery.

connected to a Gregg cannula. After the system was primed with heparinized saline solution, the tip of the cannula was inserted into the ascending aorta through the left innominate artery. Heparin sodium (Elkin-Sinn), 10,000 IU, was injected intravenously, and the roller pump was activated to replace the saline solution in the system with arterial blood. The tip of the Gregg cannula was introduced into the left main lumen and secured there with a silk tie. The roller pump was adjusted so that the left anterior descending artery pressure before introduction of the Gregg cannula was unchanged after its introduction.

Group II dogs (n = 5). A 4F catheter was placed in the left atrium for the injection of radiolabeled microspheres, and a 22-gauge catheter was inserted into the lumen of the left anterior descending artery and its tip positioned at the bifurcation of the left main artery (Fig. 2). This catheter was used for the injection of contrast medium and papaverine. An electromagnetic flow probe was attached to the left circumflex artery to measure flow through it, and a hydraulic occluder was placed on the vessel distal to the flow probe. The flow probe was connected to a flow meter that was connected to the recorder.

Group III dogs (n = 5). All branches of the aortic arch proximal to the site of aortic cross-clamp placement were ligated so that cardioplegic solution delivered to the aortic root would be directed exclusively to the native coronary arteries (Fig. 3). A hydraulic occluder was placed on the proximal left anterior descending artery, and a 22-gauge intravascular catheter was placed in the distal branch of the vessel to measure the pressure beyond the occluder. The dogs were placed on cardiopulmonary bypass with use of a roller pump (model 6002, Sarns) and a bubble oxygenator (S-100A, Shiley). They were cooled to a blood temperature of 30°C with use of a heat pump (Blanketrol 200 HL). A DLP cannula was placed in the aortic root for delivery of the cardioplegic solution and radiolabeled microspheres. An

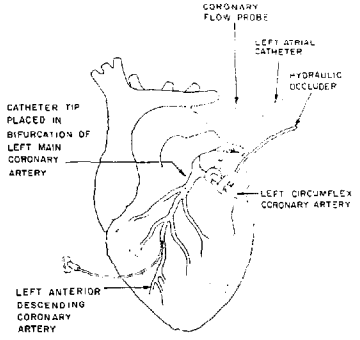

Figure 2. Animal preparation used for Group II dogs (see text for details).

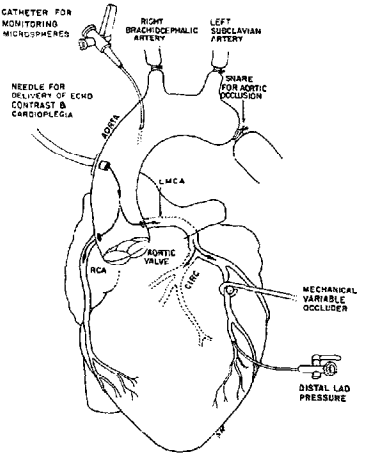

Figure 3. Animal preparation used for Group III dogs (see text for details). CIRC = left circumflex coronary artery; LAD = left anterior descending coronary artery; LMCA = left main coronary artery, RCA = right coronary artery.

18-gauge catheter was placed in the aortic root for the withdrawal of reference samples during radiolabeled microsphere injections.

Myocardial contrast echocardiography. Myocardial contrast echocardiography was performed with use of mechanical sector scanning systems. In Group I dogs, a system with an 8-MHz transducer was used (ND-256, Biosound), whereas in Group II and III dogs a system with a 5-MHz transducer was used (Mark-III, Advanced Technology Laboratories). A short-axis view of the heart was obtained at the midpapillary muscle level, and the transducer was fixed at the same level throughout the experiment by a clamp attached to the procedure table. A saline bath acted as an acoustic interface between the heart and the transducer. The control settings were kept constant throughout each experiment. In Group I dogs, a depth setting of 4 cm was used to image the left anterior descending artery bed, so that only the anterior half of the heart could be visualized on the echographic images. A depth setting of 8 cm was used for Group II and III dogs. Images were recorded on videotape with a 1.25-cm VHS recorder.

For Group I dogs, the contrast agent was made by adding 5 ml of Albunex (Molecular Biosystems) to 10 ml of 5% human albumin (Swiss Red Cross) (13). Each milliliter of Albunex consisted of approximately 450 million, 4.5-μm sonicated microbubbles. Three milliliters of this mixture was introduced through a stopcock placed proximal to the Gregg cannula (Fig. 1). In the last five Group I dogs, 2 ml of hand-agitated Renografin-saline solution with a mean microbubble size of 12 ± 7 μm was also injected at each stage (14). In Group II dogs, 2 ml of sonicated Renografin-76 was injected through the catheter placed in the left main coronary artery (Fig. 2). The microbubbles produced by this technique had a mean diameter of 6 ± 4 μm and their concentration was 500,000 ± 200,000/ml (15). In Group III dogs, the contrast agent was made by diluting Albunex (4.5 μm) in 5% human albumin to a concentration of 150,000 bubbles/ml. It was injected into the aortic root through a side port of the catheter delivering cardioplegic solution. The amount of contrast medium in each situation resulted in optimal myocardial opacification without producing any attenuation.

Computer analysis of echocardiographic images. An off-line image analysis system (Mipron, Kontron Electronics) was used for analysis of the echocardiographic images (16). In Group I and II dogs, end-diastolic images from the time of contrast injection until its disappearance from the myocardium were selected for analysis. The images were aligned by using cross correlation, as previously described (16). In brief, a region of interest is defined in a reference frame approximately equal in size to the region that is required to be aligned. A rectangular area is then defined around this region (Fig. 4A) within which the computer performs a search in the other frames for the region analogous to the region within the reference frame. Each frame to be aligned is shifted 1 pixel at a time within the search area, and the correlation coefficient between the pixels within the region of interest in the reference frame and the frame to be aligned is calculated at each position. The position at which the

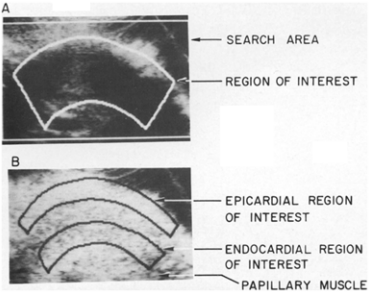

Figure 4. A, Method of image alignment. The region of the myocardium outlined in this reference frame denotes the region that needs to be aligned; the outside rectangle denotes the region in which the search has to be performed in all subsequent images (see text for details). B, Method of defining regions of interest over the anterior myocardium (imaged at a depth of 4 cm) to derive the endocardial and epicardial time-intensity curves.

correlation coefficient between the pixels in the two images is closest to 1 is taken as the best aligned position and the frame is automatically shifted and rotated to that position. In Group III dogs, in which the heart was arrested and there was no respiratory motion and image alignment was not required, all images (30 frames/s) were analyzed.

Regions of interest were placed over the epicardium and endocardium on any frame (Fig. 4B), and videointensity values in these regions were derived automatically from each frame (16). The location of these regions was determined from radiolabeled microsphere flow maps. The size of the regions of interest depended on the field depth; it was ≥600 pixels in the left anterior descending artery bed when it was imaged at a depth setting of 4 cm (Fig. 4B) and ≥200 pixels in the left circumflex bed when it was imaged at a greater depth setting. The average background activity was calculated from the four to six frames before contrast appearance and was subtracted from all subsequent frames (16). Nonlinear functions were applied to the background-subtracted plots to obtain optimal curve fitting, as previously described (16). From these functions, peak intensity of the curve, time from appearance of contrast medium in the myocardium to peak contrast effect (a measure of curve width) and area under the curve were derived (16). In Group I dogs in which large microbubbles had been injected, the initial slope of the curve was also calculated.

Measurement of myocardial flow. Myocardial blood flow in Group I and Group II dogs was determined by injecting 2×10^6 radiolabeled microspheres (Dupont Medical Products) into the left atrium (Fig. 1 and 2) just after the initiation of withdrawal of arterial blood from the left femoral artery. Ten milliliters of arterial blood was withdrawn over 90 s with use of a constant rate pump (model 644, Harvard Apparatus). In Group III dogs, 2×10^5 microspheres were injected into the cross-clamped aortic root (Fig. 3), and a reference sample was collected from the aortic root over 3 min. All microspheres were 11 μm in size and were agitated in a 4-ml solution of 0.9% saline solution and 0.01% polysorbate-80 before injection. The stopcock through which they were injected was flushed immediately after each injection.

At the end of the experiment the animal was killed, and 40 ml of Monastral blue solution (0.5% Monastral blue dye, Sigma Chemical, in phosphate buffer solution mixed with 5% dextran and 0.9% saline solution) was injected into the left main coronary artery after ligation of the proximal left anterior descending coronary artery (2). The heart was excised and the atria, great vessels and epicardial fat were discarded. A 1-cm thick slice of the left ventricle was then cut corresponding to the short-axis slice seen on echocardiography. A flow map was traced on paper showing the landmarks and the location of the left anterior descending and left circumflex artery beds.

The myocardial slice was cut into 16 approximately equal segments, and these segments were numbered clockwise starting from the junction of the left ventricular posterior and the right ventricular free walls. These numbers were also marked on the flow maps described earlier. Each segment was cut into an outer, middle and inner portion analogous to the regions of interest placed over the myocardium during echocardiographic data analysis (Fig. 4B). The samples were counted in a well counter with a multichannel analyzer (Auto-Gamma Scintillation Spectrometer model 5986). Activity spilling from one window to another was corrected, flow to each segment was calculated and the endocardial/epicardial flow ratio was derived with use of previously described equations (1,17).

Protocols. In Group I dogs, data were collected at baseline and after creation of severe left anterior descending artery stenosis. In the last five dogs, severe left circumflex artery stenosis was also created. The severity of stenosis was assessed by measuring either the distal left anterior descending artery pressure or the left circumflex artery flow. In random order, either contrast medium was injected into the left main artery or radiolabeled microspheres were injected into the left atrium. There was a 5-min delay between microbubble and microsphere injection to allow for hemodynamic equilibration. In the last five dogs, both sonicated and hand-agitated bubbles were injected at each stage.

In Group II dogs, critical stenosis was created on the left circumflex artery by tightening a micrometer attached to the hydraulic occluder until a 6-mg intracoronary injection of papaverine hydrochloride (Eli Lilly) no longer produced an increase in blood flow, as measured by the electromagnetic flow probe. Myocardial contrast echocardiography and injection of radiolabeled microspheres were performed in a random order 5 min apart before and 45 s after intracoronary injection of 6 mg of papavarine.

In Group III dogs, data were obtained at baseline and

Table 1. Range and Mean Blood Flows (ml/min per g) Achieved in All Dogs

Blood Flow	Group I		Group II:	Group III:
	LAD Bed	LCx Bed	LCx Bed	LAD Bed
Endocardial	0.00 to 1.39 (0.52)	0.04 to 0.79 (0.35)	0.21 to 2.70 (1.00)	0.09 to 1.78 (0.69)
Epicardial	0.26 to 1.35 (0.72)	0.03 to 0.83 (0.44)	0.33 to 2.70 (1.14)	0.12 to 0.82 (0.31)
Ratio	0.01 to 1.70 (0.69)	0.34 to 1.61 (0.87)	0.55 to 1.11 (0.84)	0.55 to 2.58 (1.16)

LAD = left anterior descending coronary artery; LCx = left circumflex coronary artery.

during severe left anterior descending artery stenosis. The aorta was cross-clamped, and infusion of cardioplegic solution was begun at 200 ml/min. After 1 min, when cardiac arrest had occurred, radiolabeled microspheres were injected into the cardioplegia line followed immediately by the injection of the contrast agent. Delivery of cardioplegic solution was continued for 3 min to ensure adequate washout of radiolabeled microspheres from the aortic root. Between stages, the clamp on the aorta was removed and the myocardium was perfused with blood.

Statistical analysis. All data were analyzed with use of RS/1 (Bolt, Beranek, Newman). Data were expressed as mean value ± 1 SD. Endocardial and epicardial flows and endocardial/epicardial flow ratios with echocardiographic parameters were compared with use of the paired *t* test. These parameters and their ratios were correlated with endocardial and epicardial flows and endocardial/epicardial flow ratios with use of linear regression analysis.

Results

The range of flows and endocardial/epicardial flow ratios obtained in all the dogs are listed in Table 1. The endocardial flows ranged from 0 to 2.7 ml/min per g, the epicardial flows from 0.12 to 2.7 ml/min per g, and the endocardial/epicardial flow ratios ranged from 0.01 to 2.58.

Group I dogs. Figure 5 illustrates end-diastolic images from a Group I dog after injection of sonicated albumin microbubbles at baseline (panel A) and during left anterior descending artery stenosis (panel B). At baseline, when the endocardial/epicardial ratio is 0.74, the time-intensity curves from the endocardium and epicardium are depicted in panel C. After placement of the stenosis, when the ratio is 0.32, the curves are wider; however, the change in the width is equal for both curves (panel D) despite a 58% difference in the flow ratio.

Table 2 depicts the results obtained from the left anterior descending artery bed in all Group I dogs. During injection

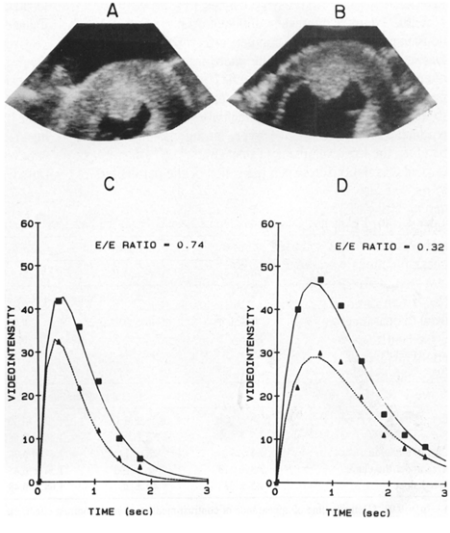

Figure 5. Data from the left anterior descending artery bed in a Group I dog. **Upper panels,** Short-axis view of the anterior myocardium imaged at a depth setting of 4 cm during peak contrast effect after intracoronary injection of sonicated microbubbles before (**A**) and after (**B**) the creation of severe left anterior descending artery stenosis. **Lower panels,** Endocardial and epicardial time-intensity curves obtained from the heart at these two stages. Data in **C** correspond to echocardiograms depicted in **A**, in which the endocardial/epicardial (E/E) ratio was 0.74; data in **D** correspond to echocardiograms in **B**, in which the ratio was 0.32 (see text for details). **Squares** denote data from the epicardial bed; **triangles** denote data from the endocardial bed.

Table 2. Blood Flow and Echocardiographic Results From the Left Anterior Descending Artery Bed in Group I Dogs

	Baseline			Stenosis		
	Endocardial	Epicardial	Ratio	Endocardial	Epicardial	Ratio
A. Small Microbubbles (11 dogs)						
Blood flow (ml/min per g)	0.75 ± 0.34	0.80 ± 0.30	0.98 ± 0.45*	0.30 ± 0.25	0.63 ± 0.32	0.40 ± 0.30*
Curve width (s)	1.54 ± 0.86	1.32 ± 0.58	1.20 ± 0.21	2.72 ± 2.21	2.10 ± 0.75	1.41 ± 1.01
Curve amplitude	30 ± 10	34 ± 17	0.97 ± 0.38	19 ± 11	26 ± 24	1.07 ± 0.40
Area under the curve	132 ± 99	128 ± 98	1.16 ± 0.69	123 ± 87	151 ± 176	1.13 ± 0.68
B. Large Microbubbles (5 dogs)						
Blood flow (ml/min per g)	0.63 ± 0.40	0.63 ± 0.16	0.95 ± 0.42‡	0.26 ± 0.22	0.49 ± 0.24	0.47 ± 0.22‡
Curve width (s)†	4.5 ± 2.6	4.1 ± 2.6	1.14 ± 0.31	3.5 ± 0.9	4.2 ± 1.0	0.84 ± 0.09
Curve amplitude	60 ± 19	57 ± 30	1.19 ± 0.37	38 ± 20	34 ± 18	1.64 ± 1.07
Area under the curve	283 ± 99	278 ± 157	1.18 ± 0.38	211 ± 95	204 ± 90	1.39 ± 1.07
Initial slope	51 ± 23	59 ± 46	1.18 ± 0.59	43 ± 13	42 ± 17	1.36 ± 1.40

*p = 0.002. †Denotes time of appearance of contrast medium to peak contrast effect. ‡p = 0.03.

of sonicated microbubbles, flow to both the epicardial and the endocardial beds was equal at baseline (Table 2A). After creation of severe stenosis, flow to the endocardium decreased more than that to the epicardium and the mean endocardial/epicardial ratio decreased from 0.98 to 0.40 (p = 0.002). The parameters of the time-intensity curves obtained from the endocardium and epicardium and the ratios of these parameters did not change significantly despite a 59% decrease in the ratio (Table 2A). Similar results were obtained with hand-agitated microbubbles in five of the dogs (Table 2B).

Table 3 depicts the results obtained from the five Group I dogs in which the left circumflex artery bed was imaged. Despite a 49% decrease in the endocardial/epicardial ratio after placement of a left circumflex stenosis, neither the parameters of the time-intensity curves nor the ratios of these parameters changed significantly (Table 3A). These parameters did not change even during the injection of hand-agitated microbubbles (Table 3B).

The correlations between the ratios of the parameters of the time-intensity curves obtained from the endocardium and the epicardium and the endocardial/epicardial blood flow ratios in Group I dogs were poor (Table 4). Even the relation between curve width and endocardial/epicardial ratios was poor. Because the appearance of the microbubbles rather than their washout may be more indicative of flow when large bubbles are used, the initial slope of the curves was also calculated during injection of large microbubbles. However, no correlation was found between endocardial/epicardial ratios and this parameter whether the left anterior descending or the left circumflex bed was imaged (Table 4).

Group II dogs. Figure 6 illustrates end-diastolic images from a Group II dog with a critical left circumflex artery stenosis after injection of contrast medium at baseline (panel A) and 45 s after intracoronary injection of 6 mg of papaverine (panel B). The left circumflex and left anterior descending artery beds show equal enhancement before injection of papaverine, whereas after papaverine injection the left anterior descending bed shows enhanced contrast effect com-

Table 3. Blood Flow and Echocardiographic Results From the Left Circumflex Artery Bed in the Group I Dogs (n = 5)

	Baseline			Stenosis		
	Endocardial	Epicardial	Ratio	Endocardial	Epicardial	Ratio
A. Small Microbubbles (11 dogs)						
Blood flow (ml/min per g)	0.48 ± 0.48	0.48 ± 0.26	0.96 ± 0.25*	0.21 ± 0.12	0.44 ± 0.14	0.49 ± 0.28*
Curve width (s)†	2.1 ± 1.1	2.2 ± 1.5	1.02 ± 0.20	1.69 ± 0.71	2.44 ± 1.06	0.71 ± 0.23
Curve amplitude	23 ± 20	14 ± 14	2.10 ± 1.30	17 ± 13	14 ± 9	1.40 ± 0.61
Area under the curve	170 ± 205	123 ± 190	1.99 ± 1.31	77 ± 53	109 ± 97	1.06 ± 0.76
B. Large Microbubbles (5 dogs)						
Blood flow (ml/min per g)	0.46 ± 0.32	0.46 ± 0.31	1.17 ± 0.30‡	0.22 ± 0.10	0.42 ± 0.18	0.58 ± 0.19‡
Curve width (s)†	4.3 ± 3.4	2.7 ± 0.8	1.46 ± 0.68	3.7 ± 2.6	4.3 ± 3.7	0.91 ± 0.10
Curve amplitude	44 ± 22	28 ± 19	1.69 ± 0.70	42 ± 18	34 ± 12	1.35 ± 0.24
Area under the curve	203 ± 119	141 ± 100	1.54 ± 0.45	189 ± 65	149 ± 40	1.40 ± 0.77
Initial slope	45 ± 38	40 ± 26	1.08 ± 0.48	37 ± 8	29 ± 13	1.48 ± 0.72

*p = 0.02. †Denotes time of appearance of contrast medium to peak contrast effect. ‡p = 0.006.

Table 4. Coefficient of Determination* Between the Ratio of Variables Derived From Time-Intensity Curves Obtained From the Endocardium and Epicardium and the Endocardial/Epicardial Blood Flow Ratio in Group I Dogs

Echocardiographic Parameter	LAD Bed		LCx Bed	
	Sonicated (11 dogs)	Hand-Agitated (5 dogs)	Sonicated (5 dogs)	Hand-Agitated (5 dogs)
Curve width†	0.00	0.35	0.10	0.23
Curve amplitude	0.24	0.03	0.18	0.16
Area under the curve	0.23	0.05	0.18	0.16
Initial slope of the curve	—	−0.05	—	−0.00

*All values represent R^2 value. †Denotes time of appearance of contrast medium to peak contrast effect. Abbreviations as in Table 1.

pared with that in the left circumflex bed. The time-intensity curves from the endocardium and epicardium in the left circumflex bed before and after papaverine are shown in panels C and D. The endocardial/epicardial flow ratio at baseline was 1.1 and decreased to 0.64 after papaverine injection. Whereas the areas under the curve decreased, they did so equally for both beds despite a >40% reduction in the flow ratio.

The results from all Group II dogs are presented in Table 5. Before papaverine injection, the endocardial and epicardial blood flows were equal, demonstrating no reduction in flow at rest despite the presence of a critical stenosis. After injection of papaverine, the decrease in flow was greater in the endocardium than in the epicardium, with a mean decrease in the flow ratio from 0.97 at baseline to 0.71 after papaverine ($p = 0.04$). However, none of the echocardiographic parameters demonstrated a significant change from baseline after papaverine injection (Table 5A). The correlations between endocardial and epicardial flows and parameters of the time-intensity curves were poor except in the case of curve amplitude and epicardial flow. The ratios of the parameters of the curves also correlated poorly with the flow ratios (Table 5B).

Group III dogs. Figure 7 illustrates end-diastolic images from one Group III dog after injection of contrast medium at baseline (panel A) and during left anterior descending artery

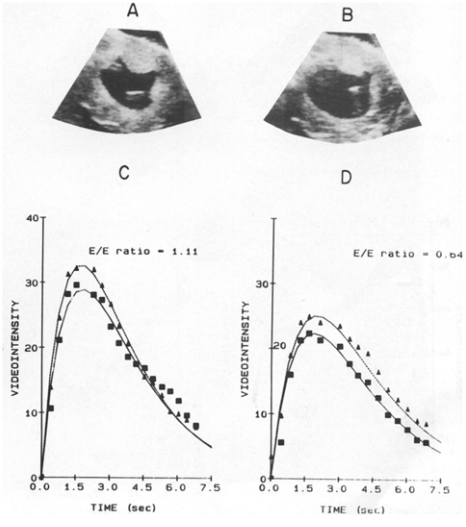

Figure 6. Data from the left circumflex artery bed in a Group II dog. **Upper panels,** Left ventricular short-axis view at a depth setting of 8 cm during peak contrast effect after intracoronary injection of sonicated microbubbles before **(A)** and after **(B)** intracoronary injection of papaverine in the presence of a critical left circumflex artery stenosis. **Lower panels,** Endocardial and epicardial time-intensity curves obtained at these stages. Data in **C** correspond to echocardiograms depicted in **A,** in which the endocardial/epicardial **(E/E)** ratio was 1.1; data in **D** correspond to echocardiograms in **B,** in which the ratio was 0.64 (see text for details). **Squares** denote data from the epicardial bed; **triangles** denote data from the endocardial bed.

Table 5. Results of Blood Flow and Echocardiographic Data From the Left Circumflex Artery Bed in Group II Dogs (n = 5)

A. Mean Data

	Before Papaverine			After Papaverine		
	Endocardial	Epicardial	Ratio	Endocardial	Epicardial	Ratio
Blood flow (ml/min per g)	1.25 ± 0.97	1.27 ± 0.87	0.97 ± 0.24*	0.75 ± 0.82	1.00 ± 0.99	0.71 ± 0.07*
Curve width (s)†	2.7 ± 1.1	2.5 ± 1.1	1.06 ± 0.11	2.1 ± 0.8	2.2 ± 1.0	0.96 ± 0.13
Curve amplitude	200 ± 73	167 ± 69	1.27 ± 0.45	149 ± 42	127 ± 46	1.22 ± 0.19
Area under the curve	192 ± 99	160 ± 91	1.35 ± 0.51	120 ± 59	109 ± 60	1.15 ± 0.13

B. Coefficient of Determination‡ Between Echocardiographic and Blood Flow Parameters

Echocardiographic variable	Endocardial Flow (normalized)	Epicardial Flow (normalized)	Endocardial/Epicardial Flow Ratio
Curve width†	0.05	0.01	0.01
Curve amplitude	0.18	0.84	0.01
Area under the curve	0.06	0.21	0.00

*$p = 0.04$. †Denotes time of appearance of contrast medium to peak contrast effect. ‡All values represent R^2 value.

stenosis (panel B). Panels C and D depict time-intensity curves from the endocardium and epicardium during these two conditions. Although the data were analyzed at 30 frames/s, they are depicted at one fifth this rate. Whereas the peak intensity and the area under the curve diminished after placement of the stenosis, the decrease was equal for both the epicardium and the endocardium despite a 32% decrease in the flow ratio.

The results from all Group III dogs are presented in Table 6. As would be expected in a nonbeating vented heart, at baseline the endocardial flow was higher than the epicardial flow. After creation of a severe stenosis, the mean

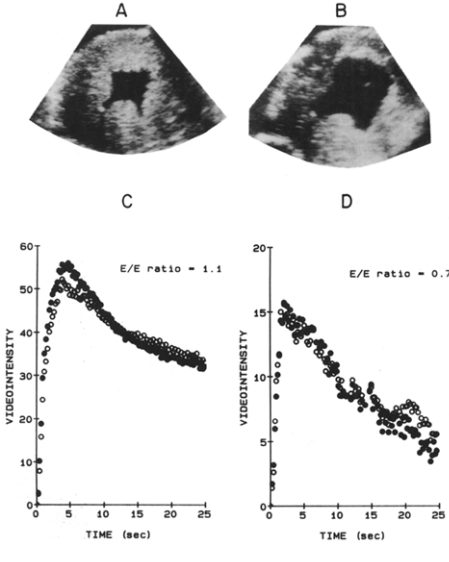

Figure 7. Data from the left anterior descending artery bed in a Group III dog where the heart was arrested and there was no motion artifact. **Upper panels,** short-axis view of the anterior myocardium imaged at a depth setting of 8 cm during peak contrast effect after injection of sonicated microbubbles into the cross-clamped aortic root before **(A)** and after **(B)** the creation of a severe left anterior descending artery stenosis. **Lower panels,** Endocardial and epicardial time-intensity plots obtained at these two stages. Data in **C** correspond to echocardiograms depicted in **A,** in which the endocardial/epicardial (E/E) ratio is 1.1; data in **D** correspond to echocardiograms in **panel B,** in which the ratio is 0.75 (see text for details). The **closed circles** denote data from the epicardial bed; the **open circles** denote data from the endocardial bed.

Table 6. Results of Blood Flow and Echocardiographic Data From the Left Circumflex Artery Bed in Group III Dogs (n = 5)

A. Mean Data

	Baseline			Stenosis		
	Endocardial	Epicardial	Ratio	Endocardial	Epicardial	Ratio
Blood flow (ml/min per g)	1.21 ± 0.39	0.75 ± 0.06	1.64 ± 0.61*	0.18 ± 0.11	0.27 ± 0.20	0.69 ± 0.10*
Curve width (s)†	4.0 ± 2.4	4.7 ± 4.6	1.02 ± 0.24	5.3 ± 6.4	6.0 ± 7.7	1.01 ± 0.24
Curve amplitude	26.6 ± 12.5	29.6 ± 14.7	0.94 ± 0.18	13.3 ± 9.0	12.3 ± 9.1	1.15 ± 0.23
Area under the curve	407 ± 258	446 ± 293	1.02 ± 0.29	173 ± 171	152 ± 163	1.50 ± 0.92

B. Coefficient of Determination‡ Between Echocardiographic and Blood Flow Variable

Echocardiographic Parameter	Endocardial Flow (normalized)	Epicardial Flow (normalized)	Ratio
Curve width†	0.0	0.01	0.10
Curve amplitude	0.51	0.74	0.06
Area under the curve	0.56	0.61	0.04

*p = 0.009. †Denotes time of appearance of contrast medium to peak contrast effect. ‡All values represent R^2 values.

endocardial flow decreased with a significant reduction in the mean endocardial/epicardial ratio from 1.6 to 0.66 (p = 0.009). None of the echocardiographic parameters demonstrated a significant change after stenosis despite an approximately 60% reduction in the flow ratios (Table 6A). The correlations between endocardial and epicardial flows and the parameters of the time-intensity curves were poor. The correlations between flow ratios and the ratios of the parameters of the time-intensity curves were also poor (Table 6B).

Discussion

Effect of microbubble size. Using myocardial contrast echocardiography, Lim et al. (7) reported lower videointensities in the endocardium during pacing in patients with coronary artery disease that were not noted at baseline. They utilized relatively large bubbles produced by hand agitation of Urografin-76. Although they documented the occurrence of ST segment depression during pacing, they did not use an independent technique to validate endocardial/epicardial flow ratios, and it is not known whether any changes in the transmural distribution of flow actually occurred in their patients.

Although Lim et al. (7) did not report the size of the bubbles used in their study, similarly produced bubbles have been reported (11,14) to have a mean size of 12 to 15 μm. Because such bubbles might get lodged in the arterioles in a manner similar to that of radiolabeled microspheres (11), it is plausible that they could be used to demonstrate the transmural distribution of flow. However, using similarly sized bubbles, we were unable in the present study to demonstrate a positive correlation between myocardial contrast echocardiography-derived parameters and endocardial/epicardial flow ratios.

The difference between our results and those of Lim et al. (7) could, in part, be explained by endocardial attenuation of the left anterior descending artery bed, which can occur when too much contrast medium is injected into the coronary circulation. This is particularly likely when hand agitation is used to prepare bubbles, because the bubble size and number cannot be standardized. Figure 8 is an example of echocardiographic images of the left anterior descending artery bed at a depth setting of 4 cm. The image before contrast injection is depicted in panel A; images after contrast injection are shown in panels B to D. Endocardial attenuation can be noted when a large number of bubbles was intentionally injected into the left anterior descending artery during normal flow (panel B), which usually dissipates in a few seconds (panel C). When a smaller number of bubbles was injected at the same flow rate, endocardial attenuation was not seen (panel D).

Because small bubbles injected into a beating heart behave similarly to red blood cells (6,12), their rate of transit through the myocardium correlates closely with blood flow. In previous studies the transit times were measured by placing regions of interest over the entire myocardial thickness and, as such, represented transmural transit times (1,2). In the present study we were unable to consistently obtain different transit times from the epicardium and endocardium in our Group I dogs receiving small microbubbles despite major differences in the flows to these regions demonstrated by radiolabeled microspheres.

Effect of location of the region of interest. When the echographic beam interrogates the left anterior descending artery bed, it samples the epicardium before the endocardium. The endocardium is therefore likely to appear attenuated if there is more contrast medium in the epicardium (Fig. 8). If, on the other hand, the echographic beam interrogates the posterior bed, the endocardium is sampled before the epicardium, in which case the epicardium should appear attenuated. Finally, if the echographic beam samples the lateral myocardium, beam attenuation can involve the epicardium and endocardium in an unpredictable manner. On

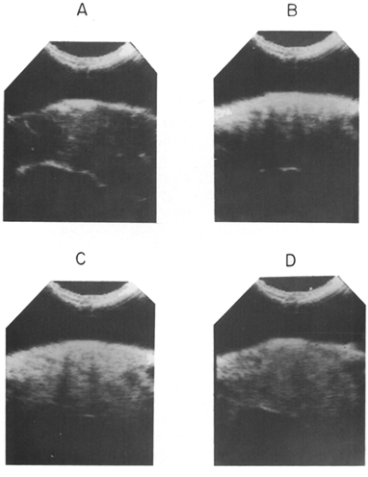

Figure 8. Effect of the amount of contrast medium injected into the coronary circulation during normal blood flow. **A,** The left anterior descending artery bed imaged at a depth setting of 4 cm before injection of contrast medium. **B,** End-diastolic frame immediately after the intentional injection of a large number of microbubbles. Endocardial attenuation is noted. **C,** End-diastolic frame 5 cardiac cycles later when the endocardial attenuation has dissipated. **D,** End-diastolic frame immediately after intracoronary injection of one third the amount of contrast medium injected in **panel B** (see text for details).

sampling myocardial beds in all three locations, we found that the results were independent of the location of the region of interest.

Effect of beating versus nonbeating heart. Our Group III dogs allowed us the unique opportunity to test two possible factors that could affect the results of our study. The first is motion of the heart. In the nonbeating heart placed on cardiopulmonary bypass there is no motion. Therefore, all frames are "naturally" aligned. In this situation, because all frames can be used to derive time-intensity curves, a temporal resolution of 30 frames/s can be achieved, which is greater than that obtained in a beating heart in which only every end-diastolic frame is analyzed. The second advantage of the nonbeating vented heart is that it has a higher endocardial than epicardial flow due to more abundant subendocardial vasculature (18). When the intracavitary pressure increases, as when the heart starts beating, the endocardial flow decreases, resulting in equalization of endocardial and epicardial flows (18). Thus, this model allowed us the opportunity to examine contrast echocardiography in the unusual situation where endocardial flow is higher than epicardial flow in the absence of ischemia. However, despite these advantages, we could not discriminate between endocardial and epicardial flows.

Effect of flow mismatch induced by coronary vasodilators. Cheirif et al. (8) reported that they could assess endocardial/epicardial flow ratio in a model of left circumflex artery stenosis after an intravenous injection of dipyridamole. This potent vasodilator has been shown to decrease this ratio as a result of "coronary steal" (19,20). In the present study, in which endocardial to epicardial flow mismatch was produced by papaverine injection, the parameters of the time-intensity curves from the endocardium and the epicardium did not correlate with endocardial and epicardial flows.

The difference in the results between the present study and those previously reported by Cheirif et al. (8) can be explained on the basis of methodology used in the two studies. Cheirif et al. reported large observer errors (16% to 27%) that almost equaled the change in the mean endocardial/epicardial flow ratio produced in their study (30%). The observer errors thus reported by these authors are significantly greater than those we and others (6,21) reported and are probably related to the methods of data analysis.

Cheirif et al. (8) used regions of interest varying in size from 63 to 86 pixels. In our Group II dogs, in which the model is comparable to the one they used, regions of interest were ≥200 pixels in size. Consequently, the signal to noise ratio in our model was at least twice that in the study by Cheirif and colleagues. Furthermore, when we analyzed the left anterior descending artery bed in our Group I dogs, our regions of interest were ≥600 pixels in size, causing our signal to noise ratio to be even higher. Cheirif et al. (8) aligned images with use of a hand-drawn template that was manually moved over each frame to find the same region of interest in different frames. In contrast, we used automatic computer cross correlation for image alignment and accepted images to be well aligned only if the R^2 values between pixels within the reference and aligned images exceeded 0.90.

We also used more precise registration between echocardiographic and radionuclide microsphere data. We created flow maps drawn from myocardial slices stained with Monastral blue dye that clearly demonstrated the myocardial segments undergoing blood flow analysis within each bed. The regions of interest placed over the myocardium during the echocardiographic image analysis were therefore nearly identical to those on the flow maps.

Possible explanations for the inability of myocardial contrast echocardiography to assess endocardial/epicardial ratio. Three possible explanations for the inability of myocardial contrast echocardiography to assess the transmural distribution of flow can be entertained. *The first is related to tissue sampling.* Unlike microbubbles, which also traverse the capillaries and venules, radiolabeled microspheres get lodged in precapillary arterioles. The venules in the epicardium drain endocardial capillaries (Fig. 9A), whereas the

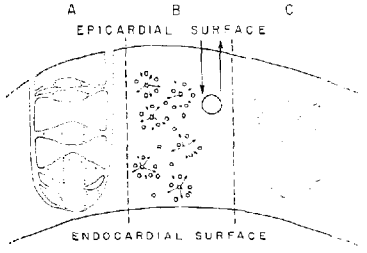

Figure 9. Diagrammatic representation of the proposed mechanisms for the inability of myocardial contrast echocardiography to assess the transmural distribution of myocardial blood flow (see text for details).

venules in the endocardium partially drain the epicardial capillaries (22). "Contamination" of the epicardial and endocardial images can result from microbubbles traversing (unlike the microspheres) regions of the myocardium into which they do not initially enter. However, if this were the only mechanism, the initial appearance of the microbubbles within the myocardium would not be affected. As can be seen from our Group 1 dogs, the initial slopes of the curves derived from the endocardial and epicardial beds did not correlate with flows to these beds when large bubbles (which should behave at least partially like microspheres) were used.

The second mechanism is related to bubble cross talk. Small bubbles (depicted as small spheres in Fig. 9B), unlike large interfaces (depicted as a larger sphere in Fig. 9B), are not reflectors but scatterers of ultrasound (23). At any given time after the injection of microbubbles, thousands of these scatterers are present in the myocardium. Scatter from one microbubble should affect that from the neighboring bubbles. This cross talk should not influence the average measurements from the entire myocardial thickness but has the potential for not allowing discrimination between the endocardium and the epicardium. However, when there is a lack of patent capillaries within the endocardial region, as may occur after reperfusion injury (the no reflow phenomenon [24,25]), the endocardial area may show less opacification because of the paucity of bubbles entering that region (26,27). In such a situation endocardial/epicardial flow ratio can be assessed with myocardial contrast echocardiography (27).

The third and final mechanism deals with flow-volume relations. The kinetics of a tracer are related to both flow and volume. If the volume is constant, the transit of the tracer is related to flow. If the flow changes, transit of the tracer can no longer be related to flow unless changes in volume are corrected (2). When ischemia is induced and the decrease in endocardial flow is disproportionate to the decrease in epicardial flow, it is likely that the endocardial blood volume also decreases as a result of fewer capillaries being open (depicted in Fig. 9C). This condition occurs as a result of either lower distending pressure or higher myocardial pressure caused by increasing intracavitary pressure induced by ischemia (18). The decreased flow coupled with decreased volume might not result in significant changes in the transit of microbubbles within the endocardium compared with the epicardium. This phenomenon is teleologically attractive, because optimal oxygen delivery during ischemia requires maintenance of the transit time of red cells through the capillaries despite decreased total flow to the endocardium.

Conclusions. In this study, using different canine models and different methods of inducing myocardial ischemia, we were unable to assess the transmural distribution of regional myocardial flow with myocardial contrast echocardiography. We have suggested possible reasons why this technique cannot be used to assess the transmural distribution of flow outside the context of the no reflow phenomenon or endocardial scar. Whereas myocardial contrast echocardiography is useful in determining relative blood flow to different myocardial beds (1–6), in its current form it cannot be used to assess the transmural distribution of myocardial flow during ischemia.

References

1. Kaul S, Kelly P, Oliner JD, Glasheen WP, Keller MW, Watson DD. Assessment of regional myocardial blood flow with myocardial contrast two-dimensional echocardiography. J Am Coll Cardiol 1989;13:468–82.
2. Keller MW, Glasheen W, Smucker ML, Burwell LR, Watson DD, Kaul S. Myocardial contrast echocardiography in humans. II. Assessment of coronary blood flow reserve. J Am Coll Cardiol 1988;12:925–34.
3. Keller MW, Spotnitz WD, Matthew TL, Glasheen WP, Watson DD, Kaul S. Intraoperative assessment of regional myocardial perfusion using quantitative myocardial contrast echocardiography: an experimental evaluation. J Am Coll Cardiol 1990;16:1267–79.
4. Tei C, Kondo S, Meerbaum S, et al. Correlation of myocardial contrast disappearance rate ("washout") and severity of experimental coronary stenosis. J Am Coll Cardiol 1984;3:39–46.
5. ten Cate FJ, Drury JK, Meerbaum S, et al. Myocardial contrast two-dimensional echocardiography: experimental examination at different coronary flow levels. J Am Coll Cardiol 1984;3:1219–26.
6. Edwards N, Jayaweera AR, Glasheen WP, Brocolli A, Spotnitz WD, Kaul S. Myocardial contrast two-dimensional echocardiography can be used to measure myocardial red blood cell transit in-vivo. Circulation 1990;82(suppl III):III-96.
7. Lim Y, Shinsuke N, Tohru M, et al. Visualization of subendocardial myocardial ischemia with myocardial contrast echocardiography in humans. Circulation 1989;79:333–44.
8. Cheirif J, Zoghbi WA, Bolli R, O'Neill PG, Hoyt B, Quinones MA. Assessment of regional myocardial perfusion by contrast echocardiography. II. Detection of changes in transmural and subendocardial perfusion during dipyridamole-induced hyperemia in a model of critical coronary stenosis. J Am Coll Cardiol 1989;14:1555–65.
9. Kaul S, Keller MW, Glasheen WP, Touchstone DA, Spotnitz WD, Gutgesell HP. Myocardial contrast echocardiography cannot be used to assess endocardial/epicardial blood flow ratio (abstr). J Am Coll Cardiol 1989;13:115A.
10. Kaul S, Glasheen WP, Sklenar J, Jayaweera AR, Villanueva FS, Spotnitz WD. The unreliability of myocardial contrast two-dimensional echocardiography in assessing the transmural distribution of blood flow (abstr). J Am Coll Cardiol 1990;15:195A.

11. Feinstein SB, Shah PM, Bing RJ, et al. Microbubble dynamics visualized in the intact capillary circulation. J Am Coll Cardiol 1984;4:595–600.
12. Keller MW, Segal SS, Kaul S, Duling BR. The behavior of sonicated albumin microbubbles within the microcirculation: a basis for their use during myocardial contrast echocardiography. Circ Res 1989;65:458–67.
13. Keller MW, Glasheen WP, Kaul S. Albunex®: a safe and effective commercially produced agent for myocardial contrast echocardiography. J Am Soc Echocardiogr 1989;2:48–52.
14. Gillam LD, Kaul S, Fallon JT, et al. Functional and pathologic effects of multiple echocardiographic contrast injections on the myocardium, brain and kidney. J Am Coll Cardiol 1985;6:687–94.
15. Keller MW, Glasheen W, Teja K, Gear A, Kaul S. Myocardial contrast echocardiography without significant hemodynamic effects or reactive hyperemia: a major advantage in the imaging of myocardial perfusion. J Am Coll Cardiol 1988;12:1039–47.
16. Jayaweera AR, Matthew TL, Sklenar J, Spotnitz WD, Watson DD, Kaul S. Method for the quantitation of myocardial perfusion during myocardial contrast echocardiography. J Am Soc Echocardiogr 1990;3:91–8.
17. Heyman MA, Payne BD, Hoffman JI, Rudolf AM. Blood flow measurements with radionuclide-labeled particles. Prog Cardiovasc Dis 1977;20: 55–79.
18. Wusten B. Biophysics of myocardial perfusion. In: Schaper W, ed. The Pathophysiology of Myocardial Perfusion. Amsterdam: Elsevier/North Holland, 1979:199–244.
19. Gross GJ, Warltier DC. Coronary steal in four models of single or multiple vessel obstruction in dogs. Am J Cardiol 1981;48:84–92.
20. Becker LC. Conditions for vasodilator-induced steal in experimental myocardial ischemia. Circulation 1978;57:1103–10.
21. Shapiro JR, Reisner SA, Amico AF, Kelly PF, Meltzer RS. Reproducibility of quantitative myocardial contrast echocardiography. J Am Coll Cardiol 1990;15:602–9.
22. Ratajczyk-Pakalska E. The coronary venous anatomy. In: Meerbaum S, ed. Myocardial Perfusion. Retroperfusion. Coronary Venous Retroperfusion. Darmstadt, Germany: Steinkopff Verlag, 1990:51–91.
23. Reisner SA, Shapiro JR, Amico AF, Meltzer RS. Contrast agents for myocardial perfusion studies: mechanisms, state of the art, and future prospects. In: Meerbaum S, Meltzer R, eds. Myocardial Contrast Two-Dimensional Echocardiography. Dordrecht, The Netherlands: Kluwer, 1989:45–59.
24. Kloner RA, Ganote CE, Jennings RB. The no-reflow phenomenon after temporary coronary occlusion. J Clin Invest 1974;54:1496–508.
25. Kloner RA, Alker KJ. The effect of streptokinase on intramyocardial hemorrhage, infarct size, and the no reflow phenomenon during coronary reperfusion. Circulation 1984;70:513–21.
26. Kemper AJ, O'Boyle JE, Cohen CA, Taylor A, Parisi A. Hydrogen peroxide contrast echocardiography: quantification in vivo of myocardial risk area during coronary occlusion and of the necrotic area remaining after myocardial reperfusion. Circulation 1984;70:309–17.
27. Villanueva FS, Glasheen WP, Sklenar J, Kaul S. Myocardial contrast echocardiography can be used to determine the success of reperfusion as well as the extent of myocardial salvage (abstr). Circulation 1991;84(suppl II):II-358.